Overall Performance of Interstage Turbine Mixed Architecture Variable Cycle Engine

LIU Bei[1,2]，NIE Ling-cong[3]，LIAO Zeng-bu[1,2]，MU Chun-hui[3]，SONG Zhi-ping[1,2]

（1. School of Mechanical Engineering，Xi'an Jiaotong University，Xi'an 710049，China；
2. State Key Laboratory for Manufacturing Systems Engineering，Xi'an Jiaotong University，Xi'an 710054，China；
3. Beijing Power Machinery Institute，Beijing 100074，China）

Abstract：To meet the supersonic cruise and subsonic cruise requirements of military air superiority fighter aircraft，a new architecture called interstage turbine mixed architecture is proposed. It contains two operating modes and eight variable cycle features. Firstly，the design concept and mission requirements are described. Then，a component-level real-time dynamic variable cycle engine model is established. Finally，the subsonic cruise fuel consumption of this variable cycle engine is optimized by a special particle swarm optimization algorithm. Compared with the fourth-generation turbofan engine，this architecture reduces the fuel consumption by 12.75% in the subsonic cruise. In addition，it also reduces some fuel consumption and improves the thrust of the intermediate state even in the supersonic cruise. Between the supersonic cruise and the subsonic cruise，it can change the bypass ratio from 0.29 to 0.82. The results show that this architecture is expected to be a variable cycle engine architecture suitable for next-generation air superiority fighters.

Key words：Variable cycle engine；Interstage turbine mixed；Component-level modeling；Particle swarm optimization；Overall performance

涡轮级间混合架构的变循环发动机总体性能研究 *

刘　备[1,2]，聂聆聪[3]，廖增步[1,2]，牟春晖[3]，宋志平[1,2]

（1. 西安交通大学 机械工程学院，陕西 西安 710049；
2. 西安交通大学 机械制造系统工程国家重点实验室，陕西 西安 710054；
3. 北京动力机械研究所，北京 100074）

摘　要：为满足军用空优战斗机的超声速巡航和亚声速巡航需求，提出了一种涡轮级间混合的变循环发动机架构，该架构包含两种工作模式和八种变循环特征。首先阐述了本架构设计理念与任务目标；然后建立了部件级实时动态变循环发动机模型；最后，在经过特有的粒子群寻优算法对变循环发动机亚声速巡航油耗寻优，对比第四代涡扇发动机油耗产生了12.75%亚声速巡航收益。此外，即使在超声速巡航点本架构也实现了一定的油耗收益和推力提升。在超声速巡航和亚声速巡航之间，可实现0.29~0.82的涵道比大范围变化。结果表明，该架构有望成为一种适用于下一代空优战斗机的变循环发动机架构。

关键词：变循环发动机；涡轮级间混合；部件级建模；粒子群寻优；总体性能

Nomenclature

VCE	Variable cycle engine		LPT	Low-pressure turbine
ITMA	Interstage turbine mixed architecture		A	Area
VABI	Variable area bypass injector		F	Uninstalled thrust
FVABI	Front variable area bypass injector		T	Temperature
RVABI	Rear variable area bypass injector		p	Pressure
MSV	Mode selection valve		W	Mass flow
CDFS	Core driven fan stage		Ma	Mach number
FLADE	Fan on blade		π	Pressure ratio
HPC	High-pressure compressor		η	Efficiency
HPT	High-pressure turbine		sfc	Specific fuel consumption

Subscripts

12	Outer bypass duct entry		design	Design value
25	CDFS entry		intrm	Intermediate state value
4	HPT entry		C	Cooling air
6	Mixer entry		CH	High-pressure compressor
8	Nozzle throat section		CL	Low-pressure compressor
t	Total		TH	High-pressure turbine
H	High pressure		TL	Low-pressure turbine
L	Low pressure		ITM	Interstage turbine mixer
a	Air		OB	Outer bypass duct
g	Gas		CB	CDFS bypass duct
aim	Aim value		cor	Corrected parameter

1　Introduction

Variable cycle engine (VCE) is a kind of engine that can change the thermal cycle through adjustable components. This concept was first proposed by General Electric in the 1960s. By adjusting the bypass ratio of the engine, VCE can get a lower specific fuel consumption (sfc) like a high-bypass ratio turbofan engine at a subsonic cruise. When supersonic cruising, it can get higher thrust like a low-bypass ratio turbofan engine, even a turbojet engine[1-3]. Therefore, it is mainly favored by supersonic airliners in the civilian market and strategic reconnaissance aircraft in the military path[4]. After the 1980s, due to the global energy crisis, people are no longer keen on the research of supersonic passenger aircraft. The research about VCE gradually transformed from civilian to military[5-6].

In 1990, General Electric developed the YF120 for the Advanced Tactical Fighter and installed it on the YF22A aircraft for the first successful test flight. Subsequently, in 2007, the United States began to launch the demonstration of the next-generation fighter and its engine.

In the planning of the next-generation fighter, there are six basic requirements for its engine that: (1) High thrust-to-weight ratio; (2) Ultra-low fuel consumption; (3) Super stealth; (4) Ultra-mobility; (5) Long life; (6) Ultra-low cost[7-8]. It means that the propulsion system of the next-generation fighter must be a kind of VCE, which can maintain superior performance at both supersonic cruise and subsonic cruise[9].

So far, the following architectures have emerged in VCE research:

(1) VCE architecture 1: Double-bypass mixed first

This architecture is currently the most widely used in domestic research on VCE. Its structure is shown in Fig. 1. Some papers suggested it is the architecture of F120, which is designed for the advanced tactical fighter F-23[9].

The third fan stage (core driven fan stage, CDFS) of this engine is connected to the high-pressure compressor (HPC), driven by the high-pressure turbine (HPT). By changing the π_{CDFS}, the CDFS adjusts the flow rate of the core engine, and changes the bypass ratio. There is a mode selection valve (MSV) to change the engine mode. The adjustable low-pressure turbine (LPT) guide can change the π_{LPT} and control the distri-

bution of HPT and LPT power. The variable area bypass injector（VABI）, namely the front variable area bypass injector（FVABI）and the rear variable area bypass injector（RVABI）is used to control the W_a of outer bypass and the working line of the fan.
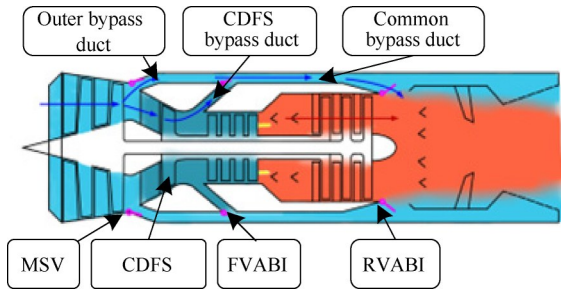

Fig. 1　Double-bypass mixed first

（2）VCE architecture 2：Separate mixing of double-bypass

The basic structure of the architecture is shown in Fig. 2. Different from the VCE architecture 1, the outer bypass and the CDFS bypass are mixed into the mixer separately in this architecture. There are two RVABIs in this architecture without FVABI.
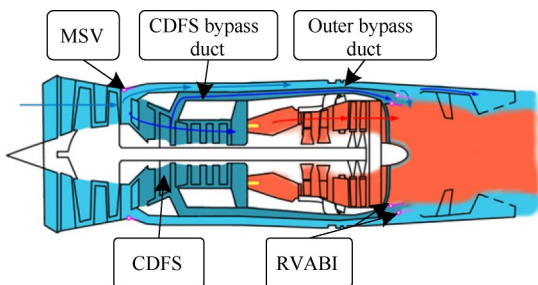

Fig. 2　Separate mixing of double-bypass

（3）VCE architecture 3：FLADE three-bypass

"Fan on blade"（FLADE）refers to a circle of small blades at the tip of the fan blade. On August 12, 2012, GE released the public promotional video material for its fifth-generation VCE[10]. As shown in Fig. 3, three bypass ducts lead from FLADE, fan, and CDFS respectively. The CDFS bypass duct and the second outer bypass duct are first merged and then mixed into the mixer after the turbine. The cold air of the first outer bypass is separately exhausted after the special-shaped nozzle. The special-shaped nozzle design can effectively block the infrared signal and enhance the stealth performance of the engine.
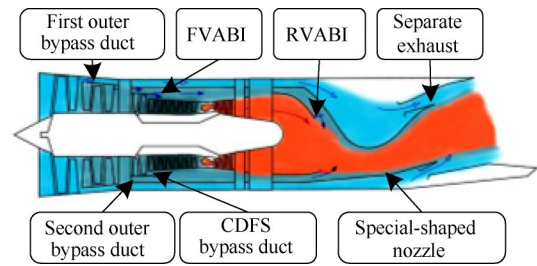

Fig. 3　FLADE three-bypass

（4）VCE architecture 4：Double-bypass split fan

On September 12, 2015, GE publicly released a video of the XA100 engine, which is designed with a 3-stage fan. The architecture is shown in Fig. 4. The third stage fan, called the split fan, is smaller in diameter than the first two stages. It makes the airflow enter the first outer. After the split fan, the airflow can enter the second outer bypass and HPC.

There are two engine modes：high thrust mode and high-efficiency mode. In high thrust mode, the airflow mainly flows into the second outer bypass. In high-efficiency mode, the air mainly flows into the first outer bypass. The first outer bypass and second outer bypass are never mixed in advance, same as architecture 2.
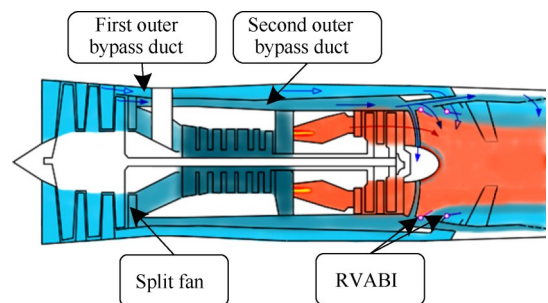

Fig. 4　Double-bypass split fan

Through the analysis, modeling, and simulation of the above 4 types of architectures, the following conclusions can be drawn：

Architecture 1 is simple, but the *sfc* decrease rate is small. During the subsonic cruise（13.5km, 0.9*Ma*）, the *sfc* decrease rate is only about 4%. Compared with architecture 1, the decrease rate of *sfc* in architecture 2 is improved, reaching about 9%, and the infrared stealth performance is optimized. However, during the subsonic cruise, the total pressure of airflow in the CDFS bypass is too high to mix with the airflow behind LPT, and the final *sfc* gains cannot make up for the

shortcomings of complex architecture.

Architecture 3 has no afterburner, and the engine pressure ratio (EPR) of the first outer bypass is smaller due to the single-stage FLADE. Therefore, the thrust per unit flow is difficult to meet the requirements of air superiority fighter jets. Architecture 4 is the same as architecture 2 basically, but the 3-stage fan has certain constraints on the higher fan speeds, which is not conducive to the decrease of *sfc* in the subsonic cruise of the engine. Therefore, it is difficult for the existing four kinds of variable cycle engines to meet the needs of supersonic cruise and subsonic cruise.

To reduce more *sfc* in subsonic cruise and guarantee supersonic cruise capability, this paper proposes an interstage turbine mixed architecture (ITMA) based on architecture 2.

2　Interstage turbine mixed VCE architecture

2.1　Mission requirements

According to the cruise points commonly used by air superiority fighters, the target operating points (shown in Table 1) for supersonic cruise and subsonic cruise are determined to be (13.5km, 1.5 *Ma*), and (13.5km, 0.9 *Ma*) respectively. And the range of the nearby working scope is determined as follows.

Table 1　Target working point

Parameter	Supersonic cruise		Subsonic cruise	
	Point	Scope	Point	Scope
High/km	13.5	12~15	13.5	11~15
Ma	1.5	1.4~1.6	0.9	0.8~0.95
F_{aim}/F_{intrm}	0.8	0.75~1.0	0.5	0.4~0.6

There are two ways to be compatible with supersonic cruise and subsonic cruise:

(1) Based on a low bypass ratio engine with excellent supersonic cruise performance, variable cycle adjustment reduces *sfc* at subsonic cruise.

(2) Based on the engine with a low *sfc* rate for subsonic cruise, variable cycle adjustment increases the unit thrust of supersonic speed.

Supersonic cruise performance is the fundamental requirement of air superiority fighters, so the former design concept is adopted.

The ITMA is shown in Fig. 5. It is a kind of double-bypass separating exhaust architecture, mainly includes eight main features and two operating modes [11]. In terms of the flow path of the ITMA, it is similar to architecture 2. To reduce the total pressure loss of the FVABI, it retains the CDFS bypass duct and the outer bypass duct without mixing.

But there are two changes as follows: (1) The ITMA uses a separate exhaust nozzle. (2) It proposes the ITM, which mixes the high-pressure airflow from the CDFS bypass duct to the turbine interstage, instead of the LPT outlet.
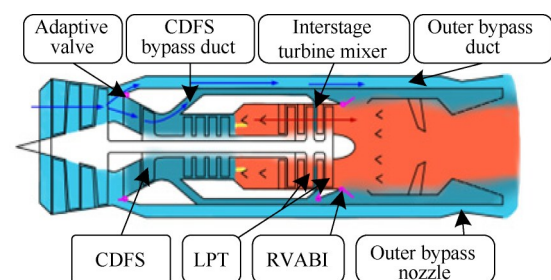

Fig. 5　Interstage turbine mixed VCE architecture

2.2　Main features

2.2.1　Multi-stage LPT configuration

Multi-stage LPT means two-stage LPT or 2.5-stage LPT (one-stage contrastive turbine and two-stage LPT)[12]. Compared with conventional one-stage LPT, this scheme can provide larger π_{LPT} and improve the power of the low-pressure shaft. When subsonic cruising, it is helpful to drive a larger airflow if the fan runs at high speed. By improving the engine airflow, the engine can achieve the goal of lower *sfc*.

2.2.2　Adjustable LPT guide vane

The adjustable LPT guide vane means that the direction of the front guide vane is adjustable. It can change the airflow direction and the critical area of the turbine guide. Within the proper range of ensuring turbine efficiency, this function can change the π_{LPT} and power of LPT to achieve a better power distribution between HPT and LPT.

2.2.3　Interstage turbine mixer

As shown in Fig. 6, the interstage turbine mixer (ITM) refers to a special component that mixes the high-pressure cold air of the CDFS bypass into the hot air between two LPT stages or between HPT and LPT. On the one hand, the component can solve the mixing

loss problem. The total pressure of the interstage turbine is closer to the CDFS bypass, which can make mixing lossless. On the other hand, this component can increase the power of the LPT by increasing the airflow of the LPT.
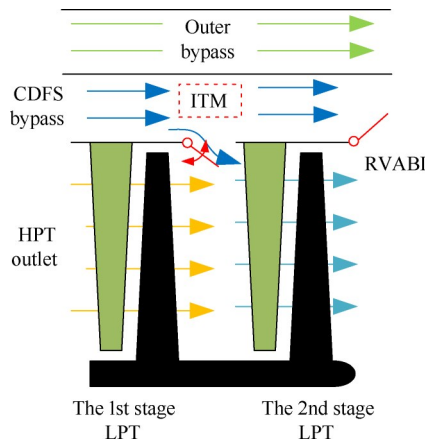

Fig. 6   Interstage turbine mixer

2.2.4   Controllable turbine cooling air

The engine bleeds some cold air from the HPC into the HPT and LPT through the pipeline. It can effectively protect turbine blades from ablation, but also reduce the overall efficiency of the turbine. When the engine is subsonic cruising, the T_{t4} is low. There is no risk of turbine ablation. According to the data analysis of the АЛ−31Ф engine, the turbine efficiency can be improved by actively reducing the cooling air. Some test data are shown in Table 2.

Table 2   Some test data of АЛ-31Ф

Data	1		2		3	
	On	Off	On	Off	On	Off
$N_{1cor}/\%$	85	82	87	81	86	83
$N_{2cor}/\%$	91	90	92	90	92	91
T_{t6}/K	851	788	918	799	884	802
$\Delta T_{t6}/K$	−63		−119		−82	
T_{t1}/K	290.61		304.30		302.63	

On the other hand, it makes all the gas of the compressor pass through the critical area of the turbine guide, which can reduce the W_{aHPC} and improve the bypass ratio.

2.2.5   Separates exhaust nozzle

There is a tail nozzle for the outer bypass duct. It makes the cold air of the outer bypass exhaust separate without mixing. This exhaust mode is mainly designed for the subsonic cruise. During the subsonic cruise, the *EPR* demand is so low that a two−stage fan can meet. By the way, this component can avoid the total pressure loss caused by the mixture. Even during the supersonic cruise, the outer bypass nozzle will not close completely. There is still cold air in the outer layer to cool the nozzle and the afterburner, to reduce infrared radiation.

2.2.6   CDFS

The design reduces the load on the low−pressure rotor, helping to increase fan speed and achieve high airflow operation. The CDFS also has adjustable guide vanes, which can adjust the airflow of the CDFS and change the bypass ratio of the engine.

2.2.7   RVABI

Because the total area of the LPT outlet and CDFS bypass is fixed, the control of RVABI can adjust their area distribution actively. It can control the CDFS duct airflow and the inner duct airflow, and active switch engine modes for subsonic cruise and supersonic cruise.

2.2.8   Adaptive valve

As shown in Fig. 7, the adaptive valve is a structure between the outer bypass duct entry and the CDFS entry. If the engine bypass ratio changes, the designed area ratio of the outer bypass duct and the CDFS entry will no longer match the bypass ratio. This must result in a greater total pressure loss.

The adaptive valve adjusts the area ratio following bypass ratio changes. It is used to optimize the flow field properly and reduce total pressure loss.
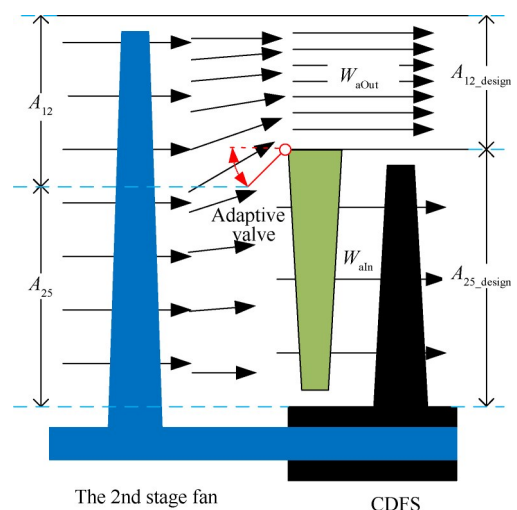

Fig. 7   Working principle of adaptive valve

2.3　Operating modes

The architecture is designed to meet the requirements of subsonic cruises and supersonic cruises. It has two operating modes: low *sfc* mode and high thrust mode. The realization process and working principle are as follows:

2.3.1　Low *sfc* mode

At the low power state (F_{aim}=50% F_{intrm}) of subsonic cruising, the engine operates in low *sfc* mode. The outer bypass nozzle is open, allowing more air to enter the outer bypass. Coordinated adjustment of RVABI and nozzle area A_8 can reduce the flow rate of the CDFS bypass, and improve the π_{LPT}. This mode can adjust the total engine exhaust pressure ratio to match the needs of the subsonic cruise, increases the total airflow W_{aFan}, and achieves maximum mass addition. In this state, the fan speed N_1 and pressure ratio π_{Fan} will rise along the working line. When the CDFS bypass pressure is higher than the pressure between the LPT stages, the air in the CDFS bypass can enter the mixer adaptively. The total pressure loss of mixing will be reduced. The LPT power will be further increased. Finally, the *sfc* is minimized.

2.3.2　High thrust mode

At the high power state (F_{aim}=100% F_{intrm}) of supersonic cruising or takeoff, the engine operates in high-thrust mode. In this mode, the engine will open the HPT cooling air to protect the blade from being ablated. The engine will actively turn down the outer culvert nozzle area, and reduce the airflow of the outer culvert. But there is still a small amount of airflow in the outer bypass for afterburner and nozzle cooling. The CDFS bypass will work as the main bypass.

In the intermediate state, the HP and LP rotors of the engine are at full speed, and the engine airflow is maximum. Due to the speed limit, it is necessary to adjust the RVABI and A_8 reasonably so that the engine burns more fuel, and increases the exhaust *EPR* and the thrust of the engine.

2.4　Component level modeling

To study these VCE characteristics, the whole engine was modeled by the component-level modeling method[13].

The framework of the component-level real-time model is shown in Fig. 8[14]. The model is comprised of component characteristics and common operating equations[15-16].

For this kind of conceptual design engine, the lack of experimental data on component properties is a common problem. So, the characteristics can only be constructed based on experience and extrapolation of conventional turbofan component properties[17]. The details will not be described due to cumbersomeness. The overall modeling approach is as follows:

(1) The parameters of the design point refer to an approximate fourth-generation turbofan engine F119[18]. These design point parameters can ensure that the ITMA engine has supersonic cruise capability. The specific parameters are shown in Table 3.

The existence of CDFS makes the LPT drive only two-stage fans and the HPT drives more rotors[19]. The π_{HPT} increases to 3.41, and the π_{LPT} reduces to 1.79. The two-stage LPT is designed for a higher fan speed and a lower *sfc* in the subsonic cruise. The optimal pressure ratio of the two-stage LPT is 3.0 to 4.0. So, the total efficiency of this LPT reduces to 0.82.

However, the thrust and *sfc* of the ITMA engine are still close to that of the F119, which shows that the design is reasonable.

(2) As for fans, compressors, turbines, combustors, and outer bypass, the characteristics are based on the general rules of the fourth-generation turbofan engines[20-21].

This component characteristic construction method is verified by the test data of the conventional turbofan engine. It can ensure that the component characteristics of the VCE conform to the basic physical laws.

(3) The influence laws of adjustable guide vanes are interpolated from the test data of several domestic engines with fully opened and fully closed guide vanes.

(4) The total pressure loss characteristic of the adaptive valve is simpler than that of turbofan engines. Compared to turbofan engines, the adaptive valve can adaptively adjust the area distribution to match the bypass ratio. So, the characteristics are constructed by ignoring the bypass ratio correction of the turbofan engine.

(5) The influence law of turbine cooling air on turbine flow and efficiency is based on the test data of the АЛ−31Ф engine. Some test data are shown in Table 2.
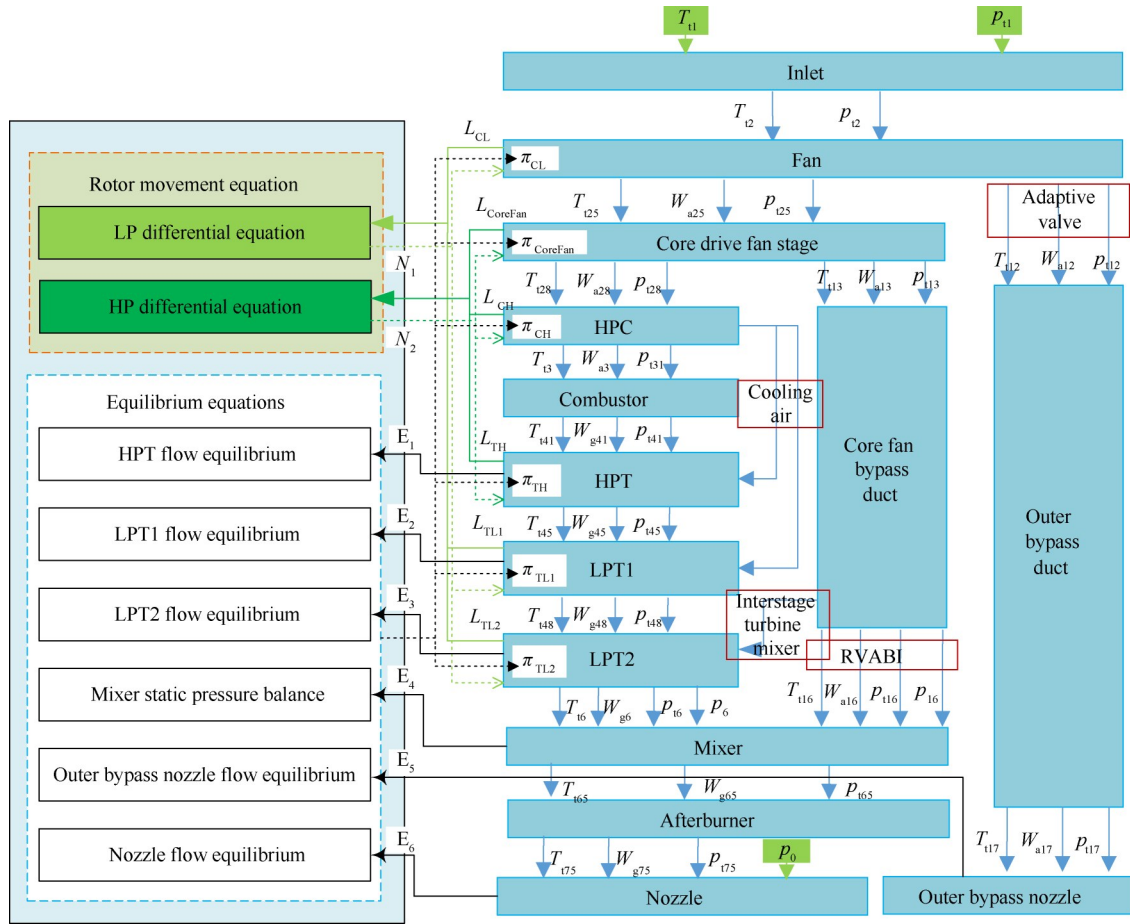
Fig. 8　Framework of the engine model

（6）The mixing characteristic of the LPT interstage mixer refers to the mixing rule of the conventional turbofan engines mixer, and the turbine cooling air mixing characteristic.

（7）Equilibrium equations are established with the relationships of pressure and mass flow balance[22]. Because of the extra components, equilibrium equations of the proposed VCE are much more complicated than the conventional turbofan engines. There are a total of 6 specific equilibrium equations, as follows.

Equilibrium equation E1 is established to represent the mass flow equilibrium on the inlet of the HPT, which can be expressed as:

$$W_{g41} + W_{aCHT} = f_{WaHT}(n_{HPTcor}, \pi_{HPT}) \qquad (1)$$

Where W_{g41} is the mass flow of the combustion chamber outlet section, W_{aCHT} is the mass flow of the HPT cooling air, n_{HPTcor} is the corrected speed of the HPT, π_{HPT} is the blowdown ratio of the HPT, $f_{WaHT}(n_{HPTcor}, \pi_{HPT})$ is the component characteristic derived mass flow.

Similar to the E1, equilibrium equation E2 is es-

tablished to represent the mass flow equilibrium on the inlet of the first-stage LPT, which can be expressed as:

$$W_{g45} + W_{aCLT} = f_{WaLT1}(n_{LPT1cor}, \pi_{LPT1}) \qquad (2)$$

Where W_{g45} is the outlet mass flow of the HPT, W_{aCLT} is the mass flow of the cooling air for the first-stage LPT, $n_{LPT1cor}$ is the corrected speed of the first-stage LPT, π_{LPT1} is the pressure ratio of the first-stage LPT, $f_{WaLT1}(n_{LPT1cor}, \pi_{LPT1})$ is the component characteristic derived mass flow.

Equilibrium equation E3 follows E1 and E2, which is devised to express the mass flow equilibrium on the inlet of the second-stage LPT and can be written as:

$$W_{g48} + W_{aITM} = f_{WaLT2}(n_{LPT2cor}, \pi_{LPT2}) \qquad (3)$$

Where W_{g48} is the outlet mass flow of the first-stage LPT, W_{aITM} is the mass flow of the interstage turbine mixer, $n_{LPT2cor}$ is the corrected speed of the second-stage LPT, π_{LPT2} is the blowdown ratio of the second-stage LPT, $f_{WaLT2}(n_{LPT2cor}, \pi_{LPT2})$ is the component characteristic derived mass flow.

Equilibrium equation E4 is a simple equal relation

<div style="display:flex">
<div>

Table 3　Design point parameters

Parameter	F119	ITMA
W_{aFan}/(kg/s)	126	126
π_{Fan}	5.0	3.2
η_{Fan}	0.85	0.85
π_{CDFS}	–	1.5
η_{CDFS}	–	0.86
W_{aCH}/(kg/s)	–	95.2
π_{CH}	5.8	6.0
η_{CH}	0.87	0.87
N_1/(r/min)	–	10200
N_2/(r/min)	–	13800
W_f/(kg/s)	–	2.59
σ_{Burn}	–	0.94
η_{Fire}	–	0.99
T_{t4}/K	–	1960
T_{t41}/K	1840	–
π_{TH}	2.64	3.41
π_{TL}	2.28	1.79
η_{TL}	–	0.82
Bypass ratio	0.29	0.32
F_{design}/kN	105.35	106.82
sfc/(kg/(N·h))	0.0852	0.0873

of the static pressure between the post−LPT and the CDFS bypass, which can be written as:

$$p_6 = p_{16} \tag{4}$$

Where p_6 is the static pressure of the LPT outlet, while p_{16} is the static pressure of the CDFS bypass outlet.

Equilibrium equation E5 is set up for the total pressure equilibrium on the outer bypass nozzle, which can be expressed as:

$$p_{tC18} = p_{t18} \tag{5}$$

Where p_{tC18} is the total pressure determined by the mass flow equilibrium, p_{t18} is the actual total pressure.

And when it comes to the main nozzle, a similar equation E6 can be obtained, which can be written as:

$$p_{tC8} = p_{t8} \tag{6}$$

Where p_{tC8} is the total pressure calculated by the mass flow equilibrium, while p_{t8} is the actual total pressure.

Finally, the component−level real−time model has been established by the component characteristics and equilibrium equations.

3　Simulation and results

As shown in Table 4, the VCE designed in this paper will be tested at two mission points. Compared with

</div>
<div>

a conventional fourth−generation turbofan engine, the performance advantages of VCE are reflected in the *sfc* and thrust. The main indicators are as follows: (1) The *sfc* at 50% intermediate states for the subsonic cruise. (2) The *sfc* at 80% intermediate states for supersonic cruise. (3) The maximum thrust at 100% intermediate state for the supersonic cruise.

Table 4　Mission points

Flight mission points	Altitude/km	Mach number
Subsonic cruise	13.5	0.9
Supersonic cruise	13.5	1.5

To obtain the optimal performance of the VCE, a performance optimization algorithm is necessary[23−24]. Therefore, a variable−step particle swarm optimization algorithm is used in this paper, which combines the particle swarm concept and variable−step search[25−26]. This algorithm has better convergence than the conventional gradient descent method in the high−dimensional non−convex optimization problem. The performance−seeking algorithm flow is shown in Fig. 9.

First, the engine runs to the target altitude and Mach number with the outer bypass duct closed. Then, the algorithm randomly generates a search particle and sets the starting point of the seeking parameters. The search particle repeats the following behaviors: (1) Adjust the search parameters of each dimension in both directions in a single step. (2) Record the optimal point in the current neighborhood. (3) Judge whether the current optimal point is at the neighborhood boundary. (4) If it is at the boundary, place the search particle at this position and repeat the previous behaviors, otherwise, it proves that there is a locally optimal point in the neighborhood, the search particle shortens the step length and repeats the previous behaviors. (5) Until the step length is short enough, the search particle has been stabilized to the local optimal point, record this particle data.

When a search particle is stabilized, the next search particle is randomly generated in the region outside twice the step length. As the number of search particles increases, the record points are gradually transformed from the local optimum to the global optimum. Until enough search particles are generated, it is consid−

</div>
</div>

ered that the lowest *sfc* state or the maximum thrust is found on a global scale.
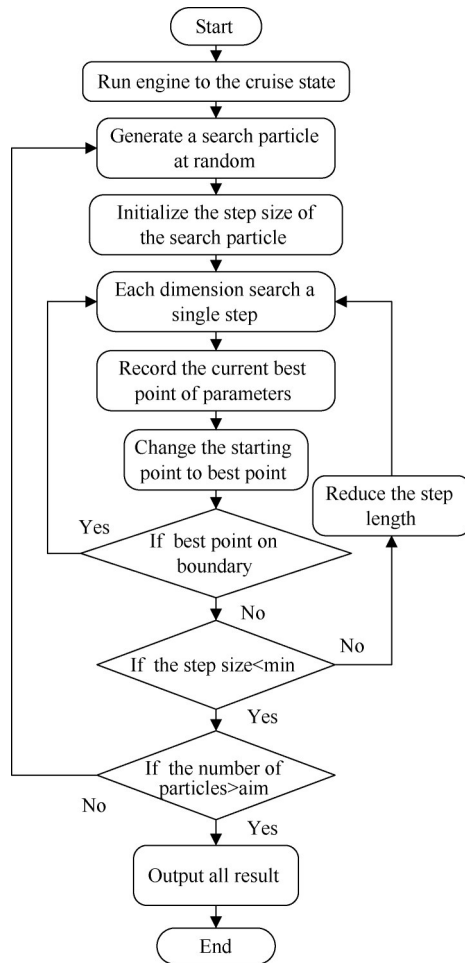

Fig. 9　Performance-seeking algorithm flow

The adjustable parameters for the sfc and thrust optimization are shown in Table 5, Where the tick means the parameter is adjustable for optimization. The fuel flow W_f is used to fix the thrust of the engine when the sfc is optimized, or improve the speed of engine rotors to the intermediate state when the thrust is optimized.

Table 5　Adjustable parameters for optimization

Parameter	*sfc*	Thrust
A_8	√	√
A_{18}	√	min
A_{16}	0.0	√
W_{aCHT}	0.0	max
W_{aITM}	√	min
Fan guide vane angle	√	√
CDFS guide vane angle	√	√
LPT1 guide angle	√	√
LPT2 guide angle	√	√

According to the above algorithm, the subsonic cruise mission point of the VCE is calculated. And the relative parameters are shown in Table 6. The *sfc* from 0.102 decreases to 0.089 realizing a gain of 12.75%. The gain comes from two sources, the increase in total engine airflow and the increase in the bypass ratio.

The two-stage LPT combined with the LPT guide vane increases the π_{LPT} from 1.85 to 2.78. The turbo interstage mixer mixes the 6.12kg/s airflow from the CDFS bypass into the LPT, which together drives the N_{1cor} up by 19.3%. The total airflow of VCE has increased by 41.2%.

The closed turbine cooling air makes the airflow of the HPC inlet reduced, and the N_{2cor} is reduced by 3.16%. The engine bypass ratio increases by 67.4%. Finally, the *sfc* has been reduced by 12.75% at the mission point of the subsonic cruise, and T_{t4} and T_{t6} have been reduced by 90.3K and 55.6K, respectively.

Table 6　*sfc* optimization for subsonic cruise

Parameter	Turbofan	ITMA	Change
N_{1cor}	0.83	0.99	19.3%
N_{2cor}	0.95	0.92	−3.16%
W_{aFan}/(kg/s)	24.5	34.6	41.2%
W_{aOB}/(kg/s)	8.1	9.5	17.3%
W_{aCB}/(kg/s)	–	6.12	–
W_{aHPC}/(kg/s)	16.4	19.0	15.9%
W_{aITM}/(kg/s)	–	6.12	–
W_{aCHT}/(kg/s)	3.5	0.0	−100 %
Bypass ratio	0.49	0.82	67.4%
π_{HPT}	2.94	3.5	19.1%
π_{LPT}	1.85	2.78	50.3%
T_{t4}/K	1363.5	1273.2	−90.3K
T_{t6}/K	865.9	810.3	−55.6K
sfc/(kg/(N·h))	0.102	0.089	−12.75%

For the supersonic cruise target of 13.5km and Mach 1.5, the target thrust of VCE is about 37436N at an 80% intermediate state. The engine mainly works with the CDFS bypass, closing the interstage turbine mixer, and leaving a small area in the outer duct for afterburner and nozzle cooling. The 80% intermediate state is a kind of near intermediate state, so the optimization interval is not much. As shown in Table 7, by adjusting the variable cycle components, an appropriate change of *EPR* can be achieved. On the premise of en-

suring that the engine thrust meets the demand，the airflow increases by 14.3% and bypass ratio increases by 47.2%.

Finally，the *sfc* has been reduced by 2.63% at the mission point of the supersonic cruise，and T_{t4} and T_{t6} have been reduced by 50.4K and 68.9K respectively.

Table 7　*sfc* optimization for supersonic cruise

Parameter	Turbofan	ITMA	Change
N_{1cor}	0.91	1.00	9.89%
N_{2cor}	0.98	0.97	−1.02%
$W_{aFan}/(kg/s)$	59.6	68.1	14.3%
$W_{aOB}/(kg/s)$	15.9	0.51	−96.8%
$W_{aCB}/(kg/s)$	−	23.0	−
$W_{aHPC}/(kg/s)$	43.7	44.6	2.06%
$W_{aCHT}/(kg/s)$	10.4	10.4	0.0%
Bypass ratio	0.36	0.53	47.2%
π_{HPT}	3.41	3.53	3.52%
π_{LPT}	1.75	2.10	20.0%
T_{t4}/K	1963.0	1912.6	−50.4K
T_{t6}/K	1230.4	1161.5	−68.9K
$sfc/(kg/(N\cdot h))$	0.114	0.111	−2.63%

The maximum thrust in the 100% intermediate state is limited by the maximum temperature of the combustion chamber and the speed of the rotor. If the maximum thrust is larger，the aircraft can balance more supersonic flight resistance，and achieve stronger supersonic cruise ability.

In this architecture，the relevant restrictions are as follows：（1）The fan relative speed does not exceed 1.01. （2）The high-pressure relative speed does not exceed 1.05. （3）The combustion chamber outlet temperature does not exceed 2150K.

The maximum thrust optimization results are shown in Table 8. The engine is running with 1.0 corrected relative speed. The total airflow is almost maximized and difficult to increase. By adjusting the variable cycle components，the engine bypass ratio can be reduced to 0.29，and the engine *EPR* increased by 7.97%. Finally，the thrust has been increased by 1206N，and improved by 2.58%. This part of thrust enhancement can improve the supersonic cruise capability of the engine effectively.

In conclusion，the simulation results show that the proposed architecture has an excellent performance in

Table 8　Thrust optimization for supersonic cruise

Parameter	Turbofan	ITMA	Change
Thrust/N	46726	47932	2.58%
N_{1cor}	1.00	1.00	0.00%
N_{2cor}	1.00	1.00	0.00%
$W_f/(kg/s)$	1.51	1.60	5.96%
EPR_{Mixed}	4.39	4.74	7.97%
$W_{aFan}/(kg/s)$	67.1	67.3	0.30%
$W_{aOB}/(kg/s)$	16.5	0.21	−98.7%
$W_{aCB}/(kg/s)$	−	14.8	−
$W_{aHPC}/(kg/s)$	50.6	52.3	3.36%
$W_{aCHT}/(kg/s)$	12.7	13.0	2.36%
Bypass ratio	0.33	0.29	−12.1%
π_{HPT}	3.42	3.40	−0.58%
π_{LPT}	1.80	1.75	−2.78%
T_{t4}/K	2103	2144	41K
T_{t6}/K	1314	1347	33K
$sfc/(kg/(N\cdot h))$	0.116	0.120	3.45%

both subsonic and supersonic cruises. It is expected to be a VCE architecture for the next generation air superiority fighter.

4　Conclusion

In this paper，the following conclusions were obtained from the study：

（1）The ITMA greatly improves propulsion efficiency at subsonic cruising speeds. During a subsonic cruise（13.5km，0.9*Ma*），the ITMA VCE can increase the bypass ratio from 0.49 to 0.82，and reduce the *sfc* by 12.75%.

（2）Features like multistage LPT，interstage turbine mixer，and adjustable turbine guide make a very positive contribution to the increases of the fan corrected speed，which enlarge the total airflow and decrease the *sfc*.

（3）Cutting off the turbine cooling airflow can efficiently decrease the HPC shaft speed. It improves the bypass ratio of the engine and reduces the total pressure loss of the bleed air in piping，thus leading to a higher propulsion efficiency when needed.

（4）This architecture also has excellent supersonic cruise performance. During a supersonic cruise（13.5km，1.5*Ma*），the adjustment of these components can still reduce the bypass ratio to 0.29 and improve the intermediate thrust to 47932N.

References

[1]　Murthy S, Curran E T. Developments in High-Speed Vehicle Propulsion Systems[M]. *Virginia*: *American Institute of Aeronautics and Astronautics*, 1996.

[2]　Allan R. General Electric Company Variable Cycle Engine Technology Demonstrator Programs[C]. *Las Vegas*: *AIAA/SAE/ASME 15th Joint Propulsion Conference*, 1979.

[3]　Johnson J. Variable Cycle Engines-The Next Step in Propulsion Evolution[C]. *Palo Alto*: *AIAA/SAE/ASME 12th Joint Propulsion Conference*, 1976.

[4]　French M, Allen C. NASA VCE Test Bed Engine Aerodynamic Performance Characteristics and Test Results [C]. *Colorado Springs*: *AIAA/SAE/ASME 17th Joint Propulsion Conference*, 1981.

[5]　Candel S. Concorde and the Future of Supersonic Transport[J]. *Journal of Propulsion and Power*, 2004, 20(1): 59-68.

[6]　Strack W, Morris J S. The Challenges and Opportunities of Supersonic Transport Propulsion Technology[C]. *Boston*: *AIAA/SAE/ASME 24th Joint Propulsion Conference*, 1988.

[7]　Tirpak J A. The Sixth Generation Fighter[J]. *Air Force Magazine*, 2009, 92(10): 38-42.

[8]　Elhefnawy N. A Sixth-Generation Fighter? An Overview of the Essential Background[J]. *SSRN*(*July* 18, 2018), 2018.

[9]　Brown R. Integration of a Variable Cycle Engine Concept in a Supersonic Cruise Aircraft[C]. *Las Vegas*: *AIAA/SAE/ASME 14th Joint Propulsion Conference*, 1978.

[10]　Chen H, Zhang H, Hu Z, et al. The Installation Performance Control of Three Ducts Separate Exhaust Variable Cycle Engine[J]. *IEEE Access*, 2018, 7: 1764-1774.

[11]　Wang R, Liu B, Yu X, et al. The Exploration of Bypass Matching Limitation and Mechanisms in a Double Bypass Engine Compression System[J]. *Aerospace Science and Technology*, 2021, 119: 107225.

[12]　Luo D, Sun X, Huang D. Design of 1+ 1/2 Counter Rotating Centrifugal Turbine and Performance Comparison with Two-Stage Centrifugal Turbine[J]. *Energy*, 2020, 211: 118628.

[13]　Wang S, Wang J, Jiang B, et al. Research of Variable Cycle Engine Modeling Technologies[C]. *Singapore*: *Proceedings of* 2016 *Chinese Intelligent Systems Conference*, 2016.

[14]　Song F, Zhou L, Wang Z, et al. Integration of High-Fidelity Model of Forward Variable Area Bypass Injector into Zero-Dimensional Variable Cycle Engine Model[J]. *Chinese Journal of Aeronautics*, 2021, 34(8): 1-15.

[15]　Li Y, Chen Y, Zhao Q. Steady State Calculation and Performance Analysis of Variable Cycle Engine[C]. *Budapest*: *9th International Conference on Mechanical and Aerospace Engineering*(*ICMAE*), 2018.

[16]　Meng X, Zhu Z, Chen M. Steady-State Performance Comparison of Two Different Adaptive Cycle Engine Configurations[C]. *Atlanta*: *AIAA/SAE/ASEE 53rd Joint Propulsion Conference*, 2017.

[17]　Xu M, Liu J, Li M, et al. Improved Hybrid Modeling Method with Input and Output Self-Tuning for Gas Turbine Engine[J]. *Energy*, 2022, 238: 121672.

[18]　陈仲光, 张志舒, 李德旺, 等. F119发动机总体性能特点分析与评估[J]. 航空科学技术, 2013(3): 39-42.

[19]　Xu Y, Chen M, Tang H. Preliminary Design Analysis of Core Driven Fan Stage in Adaptive Cycle Engine[C]. *Atlanta*: *AIAA/SAE/ASEE 53rd Joint Propulsion Conference*, 2017.

[20]　Shuang Sun, Ze-peng Wang, Xiao-peng Sun, et al. An Adaptive Compressor Characteristic Map Method Based on the Bezier Curve[J]. *Case Studies in Thermal Engineering*, 2021, 28: 101512.

[21]　Zhao R, Zhuge W, Zhang Y, et al. Study of Two-Stage Turbine Characteristic and Its Influence on Turbo-Compound Engine Performance[J]. *Energy Conversion and Management*, 2015, 95: 414-423.

[22]　Zheng J, Tang H, Chen M, et al. Equilibrium Running Principle Analysis on an Adaptive Cycle Engine[J]. *Applied Thermal Engineering*, 2018, 132: 393-409.

[23]　Chen Haoying, Zheng Qianyong, Gao Yuan, et al. Performance Seeking Control of Minimum Infrared Characteristic on Double Bypass Variable Cycle Engine[J]. *Aerospace Science and Technology*, 2021, 108: 106359.

[24]　Zhang Q, Ogren R M, Kong S. A Comparative Study of Biodiesel Engine Performance Optimization Using Enhanced Hybrid PSO-GA and Basic GA[J]. *Applied Energy*, 2016, 165: 676-684.

[25]　Bendu H, Deepak B, Murugan S. Multi-Objective Optimization of Ethanol Fuelled HCCI Engine Performance Using Hybrid GRNN-PSO[J]. *Applied Energy*, 2017, 187: 601-611.

[26]　Zhao R, Zhang H, Song S, et al. Global Optimization of the Diesel Engine-Organic Rankine Cycle(ORC) Combined System Based on Particle Swarm Optimizer(PSO) [J]. *Energy Conversion and Management*, 2018, 174: 248-259.

(编辑:白　鹭)